Journal of Asian Ceramic Societies 2 (2014) 83–96

Contents lists available at ScienceDirect

Journal of Asian Ceramic Societies

journal homepage: www.elsevier.com/locate/jascer

Review article

Recent advances in silica-alumina refractory: A review

Chaouki Sadik[a,*], Iz-Eddine El Amrani[b], Abderrahman Albizane[a]

[a] Department of Chemistry, Faculty of Science and Technology, University Hassan II, Mohammedia, Casablanca, Morocco
[b] Department of Earth Sciences, Geomaterials and Geo-Environment Team (Geo M&E), University Mohammed V Agdal, Scientific Institute, Rabat, Morocco

ARTICLE INFO

Article history:
Received 18 January 2014
Received in revised form 25 February 2014
Accepted 1 March 2014
Available online 20 March 2014

Keywords:
Clay
Sillimanite minerals
Firing
Mullite
Refractory
Thermal choc

ABSTRACT

In this article, the elaboration and the characterization of silica-alumina refractory have been reviewed. Refractory oxides encompass a broad range of unary, binary, and ternary ceramic compounds that can be used in structural, insulating, and other applications. This paper provides a historical perspective on the elaboration and the use of silica-alumina refractory, reviews applications for refractory oxides, describes typical processing routes, overviews fundamental structure–property relations, and summarizes the properties of these materials.

Contents

1. Introduction 83
2. Materials 84
3. Process routes 85
   3.1. Elaboration from clay 91
   3.2. Elaboration from sillimanite minerals and bauxite 92
   3.3. Other synthetic routes 92
4. Structure 93
5. Properties 93
6. Conclusion 95
   Acknowledgements 95
   References 95

1. Introduction

Refractory materials can be divided into several classes based on: chemical composition (acid, basic and special), method of implementation (shaped and unshaped), method of manufacture (fused and sintered), and porosity content (porous and dense). These materials are supposed to be resistant to heat and are exposed to different degrees of mechanical stress and strain, corrosion from liquids and gases, and mechanical abrasion at high temperature [1–8]. Different types of refractory materials can be synthesized according to the nature of the raw materials and the process used. The application fields of refractory are multiple and depend on the properties of each type. In fact, the performance of a refractory (good resistance to heat and thermal shock) is directly related to texture and richness of the mineral refractories, such as mullite, corundum, periclase, doloma, spinel and alumina [9,10].

Refractories are mostly used in basic metal industries. In the steel-making process by the basic oxygen furnace (BOF), the molten iron from the blast furnace is purified from the impurities including C, S, P, Mn, etc., by blowing oxygen [11]. The major characteristic requirement of these refractories is resistance to molten slag

* Corresponding author. Tel.: +212 6 45405676; fax: +212 5 23315353.
E-mail addresses: schawki37@gmail.com (C. Sadik), izdinelamrani@yahoo.fr (I.-E. El Amrani), albizane@yahoo.com (A. Albizane).

Peer review under responsibility of The Ceramic Society of Japan and the Korean Ceramic Society.

Production and hosting by Elsevier

2187-0764 © 2014 The Ceramic Society of Japan and the Korean Ceramic Society. Production and hosting by Elsevier B.V. All rights reserved.
http://dx.doi.org/10.1016/j.jascer.2014.03.001

(basic) and to the high temperature generated in the process. In the aluminum industry, the refractory property requirements are quite different from that of steel making. Although the temperature of aluminum refining and alloying process is much lower than for steel, it has the unique problem of penetration in the refractories. Hence, the refractory should be designed so that it has a nonwetting characteristic to molten aluminum [2]. In hydrocarbon industries, the refractories suffer from a high rate of abrasion due to the flow of high-velocity particles at a continuous rate. Hence, the refractory properties should be such that it should be capable of resisting the abrasion [11]. In the glass-making process, the refractories are in constant contact with the molten glass, and this poses different kinds of requirements for the refractory. Since glass in the molten state is quite fluid and tends to go through the refractory pores, the most needed characteristic should be nonporous refractories, and hence fused refractories are used in molten glass contact areas [1,6,8].

The silica-alumina refractories are materials which are increasingly demanded and whose manufacturing involves necessarily the synthesis of mullite. They have the attributes of being relatively inexpensive compared to other bricks (special carbon refractories, zircon, zirconia, fused-cast refractory). In addition, silica-alumina refractory can be used in several applications: coating of laboratory furnaces, refractory supports, thermal insulating, industrial ceramics and pottery, chemical producers, pulp and paper, food production-related industries and anything involving heat and/or hot products. This review is intended to provide a large overview of the current status of this type of refractories and to provide a summary of recent information concerning the elaboration and the characterization of mullite refractories.

2. Materials

Aluminosilicate refractories are manufactured using refractory clays, sillimanite minerals, bauxite, and mixtures of alumina and silica sand. They will refer, somewhat arbitrarily, to common crystalline compounds with melting temperatures of at least 1500 °C [2]. The major categories of traditional refractories are fire clays, high alumina, and silica. The choice of material for traditional refractory applications, as with advanced material applications, was and is based on balancing cost and performance lifetime. The ultimate use temperatures and the applications for some common refractories are summarized in Table 1 [12].

The fireclay subgroup is that having alumina content of between 25% and 45%. Because of their ease of fabrication, resistance to chemical attack, and low cost, fireclay bricks are still widely used as refractory materials. Kaolin clay, basic raw materials for the elaboration of silica-alumina refractory, is resulting from hydrothermal alteration of alkali granite. This alteration caused the kaolinization of alkali-feldspar of the granitic rock and gives an aluminous friable material (Fig. 1), rich in kaolin clay with an appreciable quantity of quartz, flakes of muscovite, and chloritized biotite. Chemically, this clay is mainly composed of alumina (29%) and silica (57%) [109].

Mullite refractory can also be produced from sillimanite minerals (Al_2SiO_5). They are the three anhydrous aluminosilicates:

Fig. 1. Career exploitation of kaolin clay of Oulmes (Moroccan Central Massif).

Fig. 2. Macroscopic sample of andalusite crystals in the region of Sidi-Bou-Othman (Morocco).

andalusite, kyanite, and sillimanite. Their ideal composition is 62.92 wt% alumina and 37.08 wt% silica [12]. However, in natural states involving significant impurities, the alumina content is usually less than 60 wt% (57.06% for Moroccan andalusite [106]). The andalusites are in the form of pink strips and whose size can reach up to 7 cm in length (Fig. 2). As the sillimanite minerals are geologically formed at high pressures (indicator mineral of metamorphism), they decompose when heated to elevated

Table 1
Compositions, ultimate use temperatures, and applications for some common silica-alumina refractory materials from [12].

Class	Material	Phases	Used temp. (°C)	Applications
Fire clay	Low heat duty	Mullite, glass, quartz	Up to 1500	Kiln linings
	High heat duty	Mullite, glass		Crucibles
High alumina	Kyanite	α-Al_2O_3, mullite, glass	Up to 1800	Metal handling
				Lab ware
Silica	Silica	Tridymite cristobalite	1650	Glass tanks crowns

Fig. 3. Crucibles and samples refractories elaborated from Moroccan geomaterials. Sintering temperature 1600 °C.

temperatures in air at 1 atm pressure [12]. The decomposition reaction can be written as [12]:

$$3Al_2O_3{\cdot}SiO_2 = 3Al_2O_3{\cdot}2SiO_2\,(\text{Mullite}) + SiO_2$$

Applications for silica-alumina refractory include insulation behind hot-face materials, furnace linings, and specialty applications such as laboratory crucibles (Fig. 3) and setters.

The refractory quality of high-alumina is usually higher than that of fireclay bearing refractories (better creep resistance and corrosion resistance). Alumina refractories contain a minimum of 60 wt% Al_2O_3, although the Al_2O_3 content can be >99% for specialty products. This type of refractories can be produced from fire clays used in combination with alumina-rich minerals such as diaspore or bauxite. Reduction of the amount of free silica (consumed in the formation of mullite) results in increased use temperature for high alumina refractories compared with fire clay refractories, up to 1800 °C for some materials. Alumina refractory is relatively low cost, and the ceramic components may be manufactured with high output using different methods, e.g. by slip casting, pressing, injection molding, etc., without the use of expensive equipment such as kilns with special controlled atmosphere. High alumina refractories can be successfully used in abrasion and erosion environments (incineration) [5,10].

Most silica refractories (crystalline or amorphous) are produced from silica-rich minerals such as quartz and flint and have SiO_2 contents of 98 wt% or higher. Because of the relatively low theoretical density of cristobalite and tridymite (2.3 g/cm^3), silica bricks are often used to construct arched furnace crowns [12]. Unlike most ceramic materials, silica bricks are resistant to creep at elevated temperature allowing them to be used for extended durations at temperatures approaching the melting temperature (Fig. 4).

The sintering of these aluminosilicate raw materials (clay, andalusite, silica sand, etc.) leads to the synthesis of Mullite ($3Al_2O_3{\cdot}2SiO_2$). The mullite is the only stable intermediate phase in the alumina–silica system at atmospheric pressure. Many of its high temperature properties are superior to those of most other metal oxide compounds, including alumina, because of its good creep resistance and high compressive and flexural strength at elevated temperature [10]. In the absence of glassy boundary inclusions, polycrystalline mullite retains more than 90% of its room-temperature strength to 1500 °C [13–22]. Another characteristic of this aluminosilicate is its excellent thermal shock resistance, low thermal conductivity and good chemical stability which may indicate a potential use in several industries such as optical, high-energy laser, ceramics and refractories [10]. The SEM micrograph of

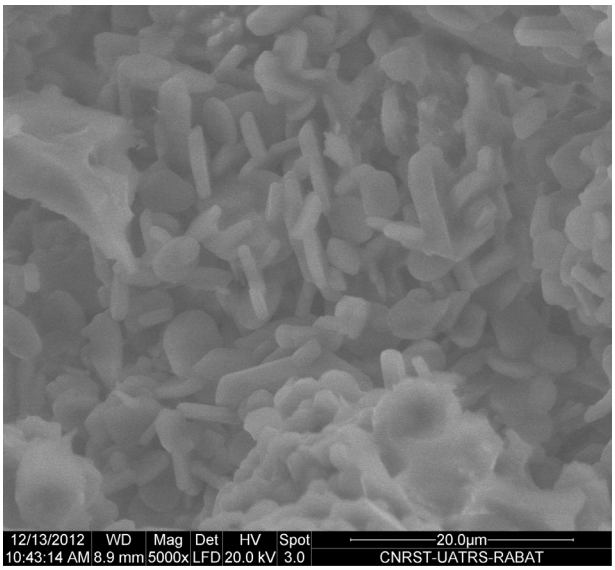

Fig. 4. Scanning electron micrograph of mixture containing pure alumina and Moroccan silica sand. Specimen was sintered at 1600 °C.

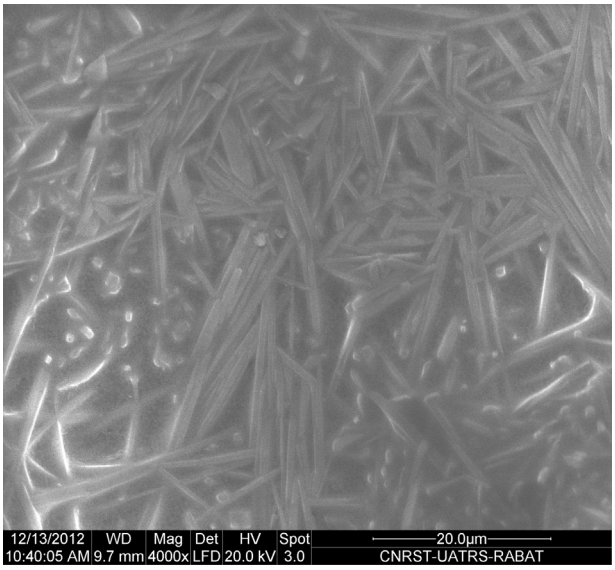

Fig. 5. Scanning electron micrograph of mullite. Mixture containing kaolin clay, cretaceous red clay and silica sand (Moroccan Geomaterials). Specimen was sintered at 1600 °C.

Fig. 5 clearly shows the mullite phase identified by its fine needle-like shape. The sample shows a homogeneous microstructure and especially richness of mullite.

3. Process routes

It is evident from a literature survey of about 100 recently published papers that the silica-alumina bricks can be used in many industrial applications requiring temperatures no greater than 1500 °C. Table 2 summarizes the process conditions, the synthesis/firing/corrosive temperatures and the characterization of the elaborated silica-alumina refractory of various research teams.

Table 2
Table comparing various research works published between 1997 and 2014.

Research team	Process and special conditions	Firing temp. (°C)	General characterization	Year of publication
Sainz et al. [24]	Microstructural evolution and growth of crystallite size of Mullite during thermal transformation of Kyanite	1600	Total transformation of kyanite to mullite: 1350–1400 °C. Below 1350 °C needle-like mullite grains are always produced.	1997
Tomba et al. [25]	Elongated mullite crystals obtained from high temperature transformation of sillimanite	1650	Total transformation of sillimanite to mullite: 1550–1600 °C.	1999
Sainz et al. [26]	XRD microstructural analysis of mullites obtained from kaolinite-alumina mixtures	1150–1700	Two kinds of mullite morphology have been observed: primary (elongated grains) and secondary (equiaxed grains) mullite.	2000
Hamidouche et al. [27]	Thermal shock behavior of mullite ceramic	–	Critical temperature difference ΔTC: 750 °C, by measuring the retained mechanical strength and the Young's modulus.	2003
Ghanbari Ahari et al. [28]	Hydration of refractory oxides in castable bond systems—II: alumina–silica and magnesia–silica mixtures	T_H 20–30	Use of Isothermal conduction calorimetry during 22 h at 20 and 30 °C. Silica tended to retard the hydration of magnesia, whereas it acted as an inert diluent when added to alumina.	2003
Kong et al. [29]	Microstructural composite mullite derived from oxides via a high-energy ball milling process	1500	The mullitization was reduced by about 200 °C after milling for 5 h.	2004
Kong et al. [30]	Effect of alkaline-earth oxides on phase formation and morphology development of mullite ceramics	1500	Mullitization temperature increased as the additives were from MgO and BaO.	2004
Viswabaskaran et al. [31]	Mullite from clay–reactive alumina for insulating substrate application	1600	MgO and boehmite were added to improve the density and decrease the sintering temperature. FS: 126 MPa, d: 3.01 (3% of MgO) FS: 120 MPa, d: 2.91 (5% of boehmite)	2004
Balmori-Ramirez et al. [32]	Dense mullite from attrition-milled kyanite and aluminum metal	1600	Silica from decomposition of kyanite, reacts with the alumina formed from oxidation of the aluminum to produce mullite.	2004
Xu et al. [33]	Synthesis, evaluation and characterization of alumina ceramics with elongated grains	1600	The elongated grain structure of alumina plays a significant role in the increment of fracture toughness.	2005
Bouchetou et al. [34]	Mullite grown from fired andalusite grains: the role of impurities and of the high temperature liquid phase on the kinetics of mullitization and consequences on thermal shocks resistance	1350	The presence of impurities in the andalusite increases the amount of the liquid phase and decreases the viscosity.	2005
Ebadzadeh [35]	Porous mullite–ZrO_2 composites from reaction sintering of zircon and aluminum	1600	The incorporation of TiO_2 improves the oxidation reaction of Al, dissociation of zircon and subsequently formation of mullite and zirconia.	2005
Ribeiro et al. [36]	High temperature mullite dissolution in ceramic bodies derived from Al-rich sludge	1250–1650	The performance of the material was evaluated through XRD, SEM/EDS, optical microscopy, and impedance spectroscopy to access the microstructural change occurring under prolonged tests (dwell times up to 100 h).	2005
Milheiro et al. [37]	Densification behavior of a red firing Brazilian kaolinitic clay	750–1150	d: 2.08; WA: 11.5%; SSA: 1 m^2/g; CS: 17.36 MPa; S: 13%	2005
Ueno et al. [38]	Water vapor corrosion of mullite containing small amount of sodium	1300–1500	After corrosion test, the samples exhibited weight gains with a rate of 6.60×10^{-6} and 8.42×10^{-5} g/cm^2 h at 1300 and 1500 °C.	2005
Torres et al. [39]	Effect of boron oxide on the microstructure of mullite-based glass-ceramic glazes for floor-tiles in the CaO–MgO–Al_2O_3–SiO_2 system	1190	Sintering of B_2O_3-containing glasses took place in 850–1050 °C. Mullite formed containing amounts of B_2O_3 >6%. For lower amounts of B_2O_3, cordierite was formed as secondary crystalline phase. The higher amount of mullite was 19.5% for the glass containing 9% of B_2O_3.	2006
Boccaccini et al. [40]	Microstructural investigations in cordierite–mullite refractories	–	Two refractory (REFO and CONC) characterized by different silica/alumina ratios, were studied. The CONC contains a larger amount of residual glassy phase than REFO, which should lead to better high-temperature mechanical properties and higher thermal shock resistance.	2005

Table 2 (*Continued*)

Research team	Process and special conditions	Firing temp. (°C)	General characterization	Year of publication
Chen et al. [41]	Microstructure and mullitization of aluminosilicate matrix in Nextel 720/aluminosilicate composites prepared by LPCVI at 550 °C	1350	Nextel 720/aluminosilicate composites were prepared by low pressure chemical vapor infiltration (LPCVI) using $AlCl_3$–$SiCl_4$–CO_2–H_2 precursor system.	2006
Montes et al. [42]	Mullite compacts obtained by colloidal filtration of alumina powders dispersed in colloidal silica suspensions	1550	Rheological optimization allows to obtain low viscosities and to reduce thixotropy and aging effects.	2006
Zawrah and Aly [43]	In situ formation of Al_2O_3–SiC–mullite from Al-matrix composites	1600	CCS: 600–690 MPa d: 2.5–3; P: 2–9% at 1600 °C	2006
Medvedovski [44]	Alumina–mullite ceramics for structural applications	–	d: 3.52–3.75 FS: 275–350 MPa	2006
Maitra et al. [45]	Zirconia–mullite materials prepared from semi-colloidal route derived precursors	1600	MgO exert a greater influence on the physico-mechanical properties of the composites than CeO_2.	2006
Diaz and Torrecillas [46]	Phase development and high temperature deformation in high alumina refractory castables with dolomite additions	1000–1400	A correlation between the microstructural phase evolution and the creep behavior with temperature was established.	2007
Santillan et al. [47]	Dense mullite from attrition milled kyanite and α-alumina	1600	Milling of kyanite and alumina for 12 h. d: 3.03	2007
Kolli et al. [48]	Elaboration and characterization of a refractory based on Algerian kaolin	1450	Different particle size fractions of kaolin. Pressure at 80 MPa d = 2.75; P = 30%	2007
Vieira et al. [49]	Mullitization kinetics from silica- and alumina-rich wastes	1300	Slate rocks and aluminum sludge. FS >100 MPa at 1285 °C.	2007
Li and Li [50]	Effects of composition and temperature on porosity and pore size distribution of porous ceramics prepared from $Al(OH)_3$ and kaolinite gangue	1600	P: 48–61% Pore size: 100 nm and 1000 nm Presence of mullite and corundum in the fired sample.	2007
Isobe et al. [51]	Gas permeability and mechanical properties of porous alumina ceramics with unidirectionally aligned pores	–	Preparation by extrusion method. P: 39%; BS: 156 MPa. The strength decreased from 156 to 106 MPa with increasing pore size from 8.5 to 38 μm. The gas permeability increased with increasing porosity and pore size.	2007
Prabhakaran et al. [52]	Microporous alumina substrate with porosity >70% by gel casting	1550	P > 70%. Average pores size of the membrane samples sintered in 1250–1550 °C varied between 0.42 and 0.56 with a maximum at 1350 °C.	2007
Wang et al. [53]	Reinforcement of mullite matrix with multi-walled carbon nanotubes (MWNTs)	1600	Addition of 5% of MWNTs led to 10% increase in BS and 78% increase in fracture toughness, compared with the monolithic mullite.	2007
Boccaccini et al. [54]	Determination of thermal shock resistance in refractory materials by ultrasonic pulse velocity measurement	–	The ultrasonic velocity technique and non-destructive characterization of thermal shock damage was demonstrated.	2007
Sahnoune et al. [55]	Algerian kaolinite used for mullite formation	1600	Formation of complete mullite occurred at 1550 °C. A density of 94% was achieved at 1600 °C and a sintering time of 4 h.	2008
Poirier et al. [56]	Analysis and interpretation of refractory microstructures in studies of corrosion mechanisms by liquid oxides	T_C 1600	The concept of local thermodynamic equilibrium to interpret the microstructures of corroded refractories. Observation of mineral zonation and composition quantification of the liquid phase at high temperature from chemical profiles established by SEM. Andalusite brick d: 2.65; P: 11.09% Bauxite brick d: 3.24; P: 16.17%	2008
Ghassemi Kakroudi et al. [57]	Effect of thermal treatment on damage mechanical behavior of refractory castables: comparison between bauxite and andalusite aggregates	1100	Mechanical properties at room temperature by tensile test.	2008
Ribeiro and Labrincha [58]	Properties of sintered mullite and cordierite pressed bodies manufactured using Al-rich anodising sludge	1350–1650	Optimal properties were obtained at 1650 °C for mullite and 1350 °C for cordierite. Mullite: S: 19%. WA: 0.7%. d: 2.5. Cordierite: S: 13%. WA: 4.2%. d: 2.07.	2008

Table 2 (*Continued*)

Research team	Process and special conditions	Firing temp. (°C)	General characterization	Year of publication
Moya et al. [59]	Mullite-refractory metal (Mo, Nb) composites	1650	Two metals were chosen to fabricate mullite–metal composites: (a) molybdenum which is thermodynamically compatible with mullite up to 1650 °C and (b) niobium, which is solid state incompatible with mullite giving rise to compounds (NbO and Nb_5Si_3) which are both electrical conductors and more oxidation resistant than the Nb metal.	2008
Djangang et al. [60]	Sintering of clay-chamotte ceramic composites for refractory bricks	1200–1350	Presence of quartz, cristobalite and mullite. The porosity increases with the chamotte content.	2008
Ouedraogo and Prompt [61]	High-temperature mechanical characterization of an alumina refractory concrete for blast furnace main trough. Part II. Material behavior	1500	Uniaxial compression, indirect tensile, creep and cyclic loading–unloading tests have been performed.	2008
Awaad et al. [62]	In situ formation of zirconia–alumina–spinel–mullite ceramic composites	1550	d: 3.3–3.5; CCS: 90–600 MPa Samples retained more than 90% of their original strength after subjected to 20 cycles of thermal shock.	2008
Prompt and Ouedraogo [63]	High temperature mechanical characterization of an alumina refractory concrete for Blast Furnace main trough	–	Results of uniaxial compression test carried out at intermediate temperature are presented and discussed.	2008
Ebadzadeh et al. [64]	Microwave-assisted synthesis and sintering of mullite	1400	Mullitization was completed after 20 min of heating with a density of about 87%.	2009
Beall [65]	Refractory glass–ceramics based on alkaline earth aluminosilicates	1650	Mullite glass–ceramics which contain considerable siliceous residual glass are the most refractory. They can be used at temperatures near 1600 °C.	2009
Ibarra Castro et al. [66]	Development of mullite/zirconia composites from a mixture of aluminum dross and zircon	1400–1500	Presence of Al_2O_3, AlN, $MgAl_2O_4$, SiO_2 and metallic Al in the fired sample.	2009
Rendtorff et al. [67]	Mullite–zirconia–zircon composites: properties and thermal shock resistance	1600	Various mullite–zirconia/zircon compositions were investigated to improve the TSR of composites produced by slip casting. The TSR improved with increasing zircon addition to 35%.	2009
Ganesh and Ferreira [68]	Influence of raw material type and of the overall chemical composition on phase formation and sintered microstructure of mullite aggregates	1725	Raw materials are ball clay, china clay and beach sand sillimanite d: 2.3–2.7; S: 15–17%	2009
Zivcová et al. [69]	Thermal conductivity of porous alumina ceramics prepared using starch as a pore-forming agent	–	λ of porous alumina prepared using different types of starch as pore-forming agents is investigated from room temperature up to 500 °C.	2009
Ghassemi Kakroudi et al. [70]	Anisotropic behavior of andalusite particles used as aggregates on refractory castables	1000–1500	The anisotropy of dilation is preserved after mullitisation of andalusite	2009
Sutcu and Akkurt [71]	The use of recycled paper processing residues in making porous brick with reduced thermal conductivity	1100	d: 1.28; λ < 0.4 W/m K Good mechanical characteristics.	2009
Rendtorff et al. [72]	Mechanical and fracture properties of zircon–mullite composites obtained by direct sintering	–	d: 3.55–4.1; P < 1% FS: 100–120 MPa	2009
Kim et al. [73]	Mullite whiskers derived from kaolin	1400	The mullite whiskers had a composition of 51.06 mol% Al_2O_3 and 48.94 mol% SiO_2, with an orthorhombic crystallographic structure.	2009
Lin and Tu [74]	Joining of mullite ceramics with yttrium aluminosilicate glass interlayers	1420	Pellets of yttrium aluminosilicate glass (Y_2O_3:Al_2O_3:SiO_2 = 30:20:50 mol%) were used as the filler interlayers (0.4 mm thick) to join two mullite substrates.	2009
Osman and Özgür [75]	Investigation of a high stable β cristobalite ceramic powder from CaO–Al_2O_3–SiO_2 system	–	A reliable β-cristobalite ceramic powder from CaO–Al_2O_3–SiO_2 ternary system was investigated at different compositions and under various sintering temperatures and sintering times.	2009
Schrijnemakers et al. [76]	Mullite coatings on ceramic substrates: stabilisation of Al_2O_3–SiO_2 suspensions for spray drying of composite granules suitable for reactive plasma spraying	–	The formation of mullite and the coating on a ceramic substrate are achieved in a single step process.	2009

Table 2 (*Continued*)

Research team	Process and special conditions	Firing temp. (°C)	General characterization	Year of publication
Mukhopadhyay et al. [77]	Pyrophyllite as raw material for ceramic applications in the perspective of its pyro-chemical properties	1350	WA: 2%; d: 2.45; S: 10.5% Presence of mullite, quartz and cristobalite at 1350 °C	2010
Ozel and Kurama [78]	Effect of the processing on the production of cordierite–mullite composite	1300	In situ cordierite mullite and layered production method.	2010
Bai [79]	Fabrication and properties of porous mullite ceramics from calcined carbonaceous kaolin and α-Al_2O_3	1550	Pore size 0.3–5 μm S: 13–17.5%; P: 20–30%; d: 2.1–2.4	2010
Zanelli et al. [80]	Phase composition of alumina–mullite–zirconia refractory materials	1500	Refractories in the Al_2O_3–SiO_2–ZrO_2 system are characterized by high mechanical strength, excellent thermal shock resistance, resistance to corrosion by alkaline compounds and low creep at high temperature.	2010
Stjernberg et al. [81]	Microstructural characterization of alkali metal mediated high temperature reactions in mullite based refractories	T_C 1400	Formation of kalsilite, nepheline and potassium β-alumina as a consequence of alkali metals migration in the brick.	2010
Di Girolamo et al. [82]	Microstructural and thermal properties of plasma sprayed mullite coatings	1600	P: 2–3% Heat capacity of recrystallized mullite coating: 1.02×10^3 J/kg K at 373 K	2010
Garcia et al. [83]	Thermal conductivity in mullite/ZrO_2 composite coatings	1000–1300	λ (K): 1.5 W/m/k at 1000 °C. At 1300 °C, K increased up to twice due to the extensive mullite crystallization.	2010
Amrane et al. [84]	Experimental study of the thermo-mechanical behaviour of alumina-silicate refractory materials based on a mixture of Algerian kaolinitic clays	1350	The behavior was analyzed through the various microstructure investigations and the presence of micro-cracking induced by the differential expansions of the multiple phases in presence. d: 2.60; P: 22.34%; S: 1.24%	2011
Abou-Sekkina et al. [85]	Phase composition of bauxite-based refractory castables	1550	Formation of the corundum and mullite.	2011
Karamanova et al. [86]	Ceramics from blast furnace slag, kaolin and quartz	1220	Good degrees of densification and high crystallinity. The BS and hardness surpass the values of traditional building and tiling materials. d: 2.12–2.34; P: 0.6–7.3 BS: 37–49 MPa	2011
Namiranian et al. [87]	Mullite synthesis and formation from kyanite concentrates in different conditions of heat Treatment and particle size	1400–1600	Total transformation of kyanite to mullite: 1500–1550 °C during 2.5 h.	2011
Rendtorff et al. [88]	Thermal shock resistance and fatigue of Zircon–Mullite composite materials	–	TSR and TFR of zircon–mullite composites were evaluated by a non destructive measurement of the elastic modulus and compared with the prediction made from the theoretical parameters (R, R‴ and RST).	2011
Prigent et al. [89]	Andalusite: an amazing refractory raw material with excellent corrosion resistance to sodium vapours	T_C 1300 °C	d: 2.25–2.61; P: 13.1–18.6% The use of mullitized andalusite particles in the matrix of alumina refractories limits the liquid phase formation during corrosion by sodium gas.	2011
Rahimi et al. [90]	Corrosion behavior of ZrO_2–SiO_2–Al_2O_3 refractories in lead silicate glass melts	T_C 1200–1350	Among three ZAS refractories tested, the most durable material was the one with the utmost baddeliyete amount, the least open porosity and the minimum eutectic mixture.	2011
Dudczig et al. [91]	Nano- and micrometre additions of SiO_2, ZrO_2 and TiO_2 in fine grained alumina refractory ceramics for improved thermal shock performance	1650	The generation of a micro-crack network after sintering due to the formation of phases with different thermal expansion coefficients and the formation and decomposition of aluminum titanate (Al_2TiO_5) before and after thermal shock exposure leads to higher strengths after thermal shock attack.	2012
Yang et al. [92]	Solid particle impact erosion of alumina-based refractories at elevated temperatures	T_{Er} 1400	Impact speed: 50 m/s Impact angle: 30–90°. The alumina-based refractories, exhibit increasing erosion resistance with increasing T °C and decreasing impact angle, with the minimum erosion rate at 1200 °C and 30° impact angle.	2012

Table 2 (*Continued*)

Research team	Process and special conditions	Firing temp. (°C)	General characterization	Year of publication
Stjernberg et al. [93]	Laboratory scale study of the degradation of mullite/corundum refractories by reaction with alkali-doped deposit materials	T_C 1350	Nepheline, kalsilite, kaliophilite, and leucite were formed as a consequence of reactions between alkali metals and the refractory bricks. The formation of these phases causes volume expansions between 20% and 25% in the brick, which accelerate degradation.	2012
Vazquez Carbajal et al. [94]	Microstructure and mechanical behavior of alumina–zirconia–mullite refractory materials	1650	MRF: 185 MPa; d: 3.5–4 Highest values of fracture toughness.	2012
Furlani et al. [95]	Possible use of waste olivine powders from a foundry process into the ceramic industry: sintering behavior of olivine, kaolin and their blends	1300	The materials fired at optimal T °C could represent an option for a possible recycling of waste olivine into the production of tiles.	2012
Stjernberg et al. [96]	Extended studies of degradation mechanisms in the refractory lining of a rotary kiln for iron ore pellet production	–	K penetrates the surface of liner bricks in much higher concentration than sodium, to a depth of several mm. Degradation is caused by simultaneous chemical reactions, resulting in the migration of eroded grains from the lining into the deposit material.	2012
Sutcu et al. [97]	Production of anorthite refractory insulating firebrick from mixtures of clay and recycled paper waste with sawdust addition	1200–1300	Mixtures with up to 30% of sawdust addition. λ and d decreased from 0.25 W/mK (1.12) to 0.13 W/mK (0.64).	2012
Gungor et al. [98]	The physical and mechanical properties of alumina-based ultralow cement castable refractories	1450	The refractory castables had strong slag penetration resistance and that the tabular alumina-based refractory had the largest specific cold crushing strength with an acceptable % of porosity.	2012
Andrews and Gawu [99]	Development of fireclay aluminosilicate refractory from lithomargic clay deposits	1400	d: 3.69–3.53; P: 2–4%; S: 10%	2012
Katsavou et al. [100]	Determination of mechanical properties and thermal treatment behavior of alumina-based refractories	1400	Use of chamotte and bauxite. Good mechanical properties.	2012
Luz et al. [101]	Effect of Al_4SiC_4 on the Al_2O_3–SiC–SiO_2–C refractory castables performance	1500	P: 15–20% Al_4SiC_4 was considered as a good alternative to carbon-containing refractories bricks.	2012
Abdi and Ebadzadeh [102]	Mullitization, microstructure and physical properties of mechanically activated andalusite sintered by microwave	1500	Mullite samples prepared from activated andalusite showed better densification with an elongated morphology.	2012
Prusty et al. [103]	Effect of MgO in the microstructure formation of zirconia mullite composites from sillimanite and zircon	1450	d: 2.71–3.25 P: 1.55–2.99%	2012
Wang et al. [104]	Phase transformation during the sintering of α-alumina and the simulated Ni-laden waste sludge	750–1250	α-Alumina interacted intensively with nickel oxide at 1000 °C	2012
Sahnoun and Bouaziz [105]	Sintering characteristics of kaolin in the presence of phosphoric acid binder	1250	Formation of alumino-phosphate. The rupture strength increased. The addition of 10 wt% of phosphoric acid decreases its calcined temperature by 200 °C.	2012
Sardy et al. [106]	Elaboration and characterization of Mullite refractory products from Moroccan andalusite	1600	Mullite formation starts as early as 1200 °C and seems almost total at 1450 °C.	2012
Martinovic et al. [107]	Cavitation resistance of refractory concrete: influence of sintering temperature	1600	The samples sintered at 1300 and 1600 °C exhibited very good cavitation resistance. d: 3.21; WA: 4.6%; P: 13.60%; CS: 274.10 MPa	2013
Sadik et al. [108]	Effect of carbon graphite on the crystallization of andalusite	1400	Mixtures of natural geomaterials (clay, sand, marl). Adding of carbon graphite. Good mechanical and thermal performance; d: 2.86.	2013
Sadik et al. [109]	Effect of andalusite rich schist grain size and the addition of metallic aluminum powder on the properties of silica–alumina refractory	1450	The use of andalusite rich schist as aggregates (1000–2000 μm) could improve the mechanical properties. The FS increased from 39.10 to 54.16 MPa. The pyroscopic temperature increased from 1400 to 1450 °C.	2013

Table 2 (*Continued*)

Research team	Process and special conditions	Firing temp. (°C)	General characterization	Year of publication
C. Sadik et al. [110]	Production of porous firebrick from mixtures of clay and recycled refractory waste with expanded perlite addition	1600	The samples maintained the shape without undergoing any deformation up to 1600 °C. The use of expanded perlite decreased the fired density of the bricks down to 1.55.	2013
Isobe et al. [111]	Preparation and gas permeability of the surface-modified porous Al_2O_3 ceramic filter for CO_2 gas separation	1000	Pore size: 74 nm P: 40%	2013
Shirasaka et al. [112]	Analysis of gas permeability of porous alumina powder compacts	800	P: 35–45%	2013
Meng and Peng [113]	Effects of in situ synthesized mullite whiskers on flexural strength and fracture toughness of corundum–mullite refractory materials	–	The optimum process parameters: sintering temperature: 1350 °C The holding time: 2 h V_2O_5 addition: of 5%	2013
Boussois [114]	Characterization of textured ceramics containing mullite from phyllosilicates	1400	Organized ceramics are obtained from kaolinite and muscovite suspensions and shaped by aqueous tape casting or centrifugation.	2013
Bai et al. [115]	Fabrication and properties of cordierite–mullite bonded porous SiC ceramics	1300–1450	The surface of SiC was oxidized to SiO_2. With further increasing the temperature, SiO_2 reacted with $Al(OH)_3$ and MgO to form cordierite–mullite.	2013
Sembiring et al. [116]	Synthesis and characterization of gel derived mullite precursors from rice husk silica	1400	Mullite formation started at 1150 °C, and its abundance increased rapidly with an increase in temperature from 1150 to 1350 °C (30.9–67.7%).	2013
Jing et al. [117]	Fabrication and properties of SiC/mullite composite porous ceramics	1250–1450	Preparation from a mixture of calcined kaolin, aluminum hydroxide, silicon carbide and graphite. Calcined kaolin/$Al(OH)_3$ ratio = 1:1.5, FS: 48.14 MPa; P: 33.97% 15% graphite. FS: 27.26 MPa; P: 48.80%.	2014
Ieva Zake-Tiluga et al. [118]	Highly porous corundum–mullite ceramics – structure and properties	–	Addition of 3.7% of SiO_2 increased the bending strength by up to 250%. The best mechanical properties were achieved with samples that were modified with SiC and Si_3N_4 nanopowders.	2014
Rendtorff et al. [119]	Dense mullite-zirconia composites obtained from the reaction sintering of milled stoichiometric alumina zircon mixtures by SPS	–	The microstructure and mechanical properties obtained were comparable to the ones obtained by other processing routes.	2014
Sedaghat et al. [120]	Microstructure development and phase evolution of alumina–mullite nanocomposite	1750	The relative density of alumina–mullite that was sintered at 1650 °C for 2 h was obtained as 98.7%. After sintering at 1750 °C for 2 h, the mullite was decomposed.	2014

d: density (g/cm^3); P: porosity (%); S: shrinkage (%); WA: water absorption (%); FS: flexural strength (MPa); SSA: specific surface area; CS: compressive strength (MPa); CCS: cold compressive strength; λ: thermal conductivity; MRF: resistance to fracture; TSR: thermal choc resistance; T_C: temperature of corrosion; T_{Er}: temperature of erosion; T_H: temperature of hydration; BS: bending strength (MPa).

3.1. Elaboration from clay

Clays are ubiquitous constituents of the Earth's crust that serve as raw materials for traditional ceramics. When mixed with water, clays develop plasticity and can be shaped easily and reproducibly [23]. When heated, clays undergo a series of reactions that ultimately produce crystalline mullite and a silica-rich amorphous phase [48]. Beyond the structure and properties of clays, the science that developed to understand traditional ceramics continues to serve as the framework for the study of advanced ceramics.

Kolli et al. [48] have elaborated refractory material from kaolin (39.87% of SiO_2; 38.36% of Al_2O_3). The calcined grog at 1350 °C/1 h, was used as aggregates with granulometric distribution composed of fine fraction (size: 100–250 μm) and coarse fraction (size: 1000–2500 μm). Crude kaolin (size <75 μm) was also used as a binder. Samples shaped by uniaxial pressure at 80 MPa were fired between 1250 and 1450 °C. An X-ray diffraction (XRD) analysis showed the presence of mullite and silica. The porosity is about 30% and the density is equal to 2.75 g/cm^3. Thermal shock tests showed that the refractory samples present good thermal shock resistance. A year later, Sahnoune et al. [55] have elaborated mullite through reaction sintering of kaolinite and high purity alumina. Formation of complete mullite occurred at 1550 °C. Kaolin–phosphoric acid mixtures (5; 10 and 15 wt% of acid) have been investigated by Sahnoun and Bouaziz [105]. During the maturation and the sintering processes, acid reacts with aluminum of kaolin (29.83%) to give a new phase of aluminophosphate. The obtained rupture strength is higher than that of those made with only kaolin. The porosity decreases with both the sintering temperature rise and the addition of phosphoric acid in the mixture. The addition of 10 wt% of phosphoric acid to the kaolin decreases its calcined temperature by 200 °C.

Andrews and Gawu [99] have studied the production of refractory material from lithomargic clay deposit. Lithomargic clay underlying bauxite deposits in Ghana result from incomplete bauxitisation process. The lithomargic clay consists mainly of kaolinite and gibbsite (42.2% of Al_2O_3; 50.3% of SiO_2). The results

show that the linear firing shrinkage values were within limits acceptable for refractory clays. The cold crushing strength increases as temperature increased to 1400 °C and with increasing binder content. This study indicates that lithomargic clay under lying bauxite deposits could be used to produce fire clay aluminosilicate refractories. Bai [79] has used calcined carbonaceous kaolin (35.97% of Al_2O_3) and α-Al_2O_3 powders to prepare porous mullite ceramics using graphite as pore former. For the purpose of comparison, porous mullite ceramics was also fabricated from the uncalcined carbonaceous clay incorporated with α-Al_2O_3 powders. Mullitization was both nearly complete at 1500 °C. Li and Li [50], have elaborated porous corundum-mullite ceramics from $Al(OH)_3$ and kaolinite gangue by the in situ decomposition pore-forming technique. The porosity of the sample increases with increasing $Al(OH)_3$ content. Micropores with maximum diameter of 100 and 1000 nm exist in the structure.

Djangang et al. [60], have elaborated composites based on clay-chamotte. These composites containing various quantities of chamotte (0–50 wt%) were sintered at 1200–1350 °C. XRD indicated the presence of quartz, cristobalite and mullite. SEM observations revealed very heterogeneous microstructures where porosity is weakly distributed and large pores are entrapped at the vicinity of large chamotte and quartz grains. Nevertheless, characteristics of materials are sufficient for the manufacturing of industrial kilns, used at temperature not exceeding 1200 °C. In 2013, Sadik et al. [109] have elaborated refractory from silica–alumina geomaterials related to granitoids and their direct surrounding rocks (kaolin clay and andalusite rich schist). The use of andalusite rich schist as aggregates (size: 1000–2000 μm) could improve the mechanical properties of synthesized refractory. The flexural strength increased from 39.10 to 54.16 MPa. The pyroscopic temperature increased from 1400 to 1450 °C. Production of porous and lightweight bricks with acceptable flexural strength is accomplished. Expanded perlite was used as an additive to produce the pores [110]. The results obtained showed that the tested samples maintained their shape without undergoing any deformation up to 1600 °C. The use of expanded perlite decreased the fired density of the bricks down to 1.55 g/cm^3. Ganesh and Ferreira [68] have prepared dense mullite aggregates with varied alumina contents (47–70%) by a conventional dry-powder pressing technique followed by heat treatments at temperatures ranging from 1450 to 1725 °C. Different types of clays (ball clay, 34.2% of Al_2O_3; china clay, 35.16% of Al_2O_3), beach sand sillimanite (BSS, 53.5% of Al_2O_3) and a high purity of aluminum hydroxide (64.5% of Al_2O_3) were used as starting materials. Mullite aggregates obtained through a double-stage heat treatment process exhibited better sintered properties in terms of bulk density, apparent porosity, water absorption capacity and higher mullite contents in comparison to those obtained following a single-stage firing process. Kim et al. [73] have synthesize short mullite whiskers prepared by firing compacts (1300–1400 °C for 15 h) of kaolin and $NH_4Al(SO_4)_2{\cdot}12H_2O$ powders, with a small addition of $NaH_2PO_4{\cdot}2H_2O$ (0.8, 1.5 wt%). The elaborated mullite whiskers had a composition of 51.06 mol% of Al_2O_3 and 48.94 mol% of SiO_2, with an orthorhombic crystallographic structure.

Karamanova et al. [86], have elaborated ceramic from blast furnace slag (9.3% of Al_2O_3), kaolin (33.2% of Al_2O_3) and sand (0.2% of Al_2O_3). The obtained ceramics are characterized with a narrow sintering interval at 1200–1220 °C, good degrees of densification and show high crystallinity (pyroxene and anorthite solid solution). The hardness and the bending strength increase with slag amount. The basic research of Furlani et al. [95], realized in 2013, aims to evaluate the possible recycling of olivine (0.96% of Al_2O_3), a by-product of a foundry process, into the ceramic industry. Olivine powders were milled alone or blended with 20, 40, 60 and 80 wt% of high-grade kaolin (36.84% of Al_2O_3) by attrition milling to obtain powders of different compositions. The materials fired at their optimal temperature (1150–1200 °C) could represent an option for a possible recycling of waste olivine into the production of tiles. Production of porous anorthite refractory firebricks from mixtures of clays (59% of SiO_2; 38.5% of Al_2O_3), recycled paper processing waste, and sawdust addition are investigated by Sutcu et al. [97]. Thermal conductivities of the samples produced from fireclay and recycled paper waste decreased from 0.25 W/mK (1.12 g/cm^3) to 0.13 W/mK (0.64 g/cm^3) with decreasing density. Samples were stable at high temperatures up to 1100 °C, and their cold strength was sufficiently high.

3.2. Elaboration from sillimanite minerals and bauxite

Bouchetou et al. [34], have studied the mullitization and microstructure of mullite grown from fired andalusite grains (61% of Al_2O_3). The study shows that the presence of impurities (iron and alkalis) in the andalusite increases the amount of the liquid phase. The mullitization kinetics depends on the andalusite grain size, the chemical composition and the amount of the liquid phase. Santillan et al. [47] have studied the effect of attrition milling on the decomposition of kyanite and its reaction with α-alumina to form stoichiometric mullite. Kyanite-alumina mixes were attrition milled for times from 1 h to 12 h. With increasing milling time, the kyanite decomposition was accelerated and secondary mullite formation from the reaction between the rejected silica and the added alumina was enhanced. Milling reduced the decomposition expansion from +15.0% to +0.1% and the final contraction or densification from +2.5% to −13.7%. Abou-Sekkina et al. [85] have studied the phase composition of bauxite-based refractory castables. The samples are composed of 90 wt% well-graded (coarse, medium, and fine) bauxite aggregate, 10 wt.% binding matrix and adequate amount of distilled water. The XRD patterns indicated the formation of the corundum phase along with mullite phase in all of bauxite-based castable samples. The SEM micrographs show densely packed microstructures with an abundant of corundum grains of comparable sizes, rounded and sub-rounded, homogeneously embedded in the matrix. Needle-shaped mullite crystals are present in the structure.

The process of mullitization of kyanite concentrate was studied again at different conditions of heat treatment (1400–1600 °C; 0.5–3.5 h) and of particle size of raw materials (38–300 μm) by Namiranian and Kalantar [87]. The results of microstructure (shape, distribution and size of the grains) and phase evolution studies by SEM and XRD showed that total transformation of kyanite to mullite takes place between 1500 and 1550 °C during 2.5 h. At temperatures below 1500 °C need-like mullite grains are always produced. Elaboration and characterization of mullite refractory products from Moroccan andalusite was studied by Sardy et al. [106] between 1200 °C and 1600 °C. Mullite formation starts as early as 1200 °C and seems almost total at 1450 °C. Mullitization, microstructure and physical properties of mechanically activated andalusite (44.99% of Al_2O_3) sintered by microwave was studied by Abdi and Ebadzadeh [102]. XRD results revealed that andalusite peaks disappeared after 60 h of milling and the peaks of alumina were observed. Mullite samples prepared from activated andalusite showed better densification with an elongated morphology.

3.3. Other synthetic routes

Mullite powders prepared by advanced processing, e.g. sol-gel, precipitation, hydrolysis, spray pyrolysis, chemical vapor deposition (CVD) techniques are designated ‘chemical-mullite’ [10]. The fabrication of porous SiC/mullite composite ceramics has been

studied by Jing et al. [117]. The products were prepared from a mixture of calcined kaolin (35.97% of Al_2O_3), aluminum hydroxide (99.9%), silicon carbide, and graphite. The mixture was heated at 1250–1450 °C to produce pores by burning graphite and bond the SiC particles by reaction-derived mullite. The results show that when the mass ratio of calcined kaolin/$Al(OH)_3$ is 1:1.5, and in the absence of graphite, the flexural strength and the open porosity of the composites were 48.14 MPa and 33.97%, respectively. However, when 15% graphite was added to the above composition, a flexural strength of 27.26 MPa was achieved at an open porosity of 48.80%. Highly porous corundum–mullite ceramics have been elaborated by Zake-Tiluga et al., by slip casting [118]. The aim was to improve the mechanical properties of porous corundum ceramics by adding various types of SiO_2 source (SiO_2, SiC and Si_3N_4). Pores were formed using aluminum's reaction with water. It was found that the bending strength of the material can be improved and relatively high porosity retained by producing corundum–mullite composites. Addition of 3.7 wt% of SiO_2 source increased the bending strength by up to 250% in comparison with unmodified corundum ceramics. The apparent porosity decreased by up to 8%. If the amount of SiO_2 source was increased from 3.7 to 7.3 wt%, the bending strength decreased. The best mechanical properties were achieved with samples that were modified with SiC and Si_3N_4 nanopowders. This is due to better dispersion in Al_2O_3 matrix.

Cordierite–mullite bonded porous SiC ceramics were prepared by an in situ reaction bonding technique using a silicon carbide, aluminum hydroxide, MgO, and graphite as starting materials [115]. The starting materials were mixed in different ratios and heated between 1300 and 1450 °C to obtain good mechanical properties. The pores in the ceramics were formed by burning graphite and by stacking particles of SiC and $Al(OH)_3$. The surface of SiC was oxidized to SiO_2 at high temperature, and fine Al_2O_3 grains produced by the decomposition of aluminum hydroxide. With further increasing the temperature, SiO_2 reacted with $Al(OH)_3$ and MgO to form cordierite–mullite. The results show that when 4.5 wt% MgO was added, in the absence of graphite, the flexural strength and the open porosity of the porous SiC ceramics were 78.71 MPa and 21.63%, respectively. In addition, with 30% of graphite, a flexural strength of 41.29 MPa was achieved at an open porosity of 42.11%. The sol–gel synthesis and characterization of mullite precursor derived from rice husk silica and aluminum nitrate hydrate [$(Al(NO_3)_3{\cdot}9H_2O$] has been investigated by Sembiring et al. [116]. FTIR results showed the presence of Si—O—Si, Al—O—Al, and Si—O—Al functional groups, which were associated with mullite, corundum, quartz, and cristobalite, as verified by XRD analysis. It is concluded that mullite formation started at 1150 °C, and its abundance increased rapidly with an increase in temperature from 1150 to 1350 °C, resulting in increased phase content from 30.9 to 67.7 wt%. This finding demonstrated that rice husk silica is a potential alternative raw material for the production of mullite ceramic. Dense mullite-zirconia composites obtained from the reaction sintering of milled stoichiometric alumina-zircon mixtures by SPS have been studied by Rendtorff et al. [119]. The main objective is to obtain dense (porosity under 0.5%) polyphasic ceramics belonging to the Al_2O_3—SiO_2—ZrO_2 system by SPS sintering of high energy powders milled drily; the stoichiometric (54.45:45.54 zircon–alumina, weight basis) mixture was explored. The mechanical pretreatment used resulted in a homogeneous dry mixture with a partial (≈20%) zircon dissociation, apparently enhanced by the alumina presence. This together with the posterior SPS processing permitted to obtain fully dense ceramic composites at a very low temperature (1300 °C) without the requirement of any additive. The reactions from alumina zircon mixtures to mullite zirconia occur 200 °C below conventional processing routes and at least 50 °C below the reported SPS based materials processed from un-milled mixtures. Microstructure development and phase evolution of alumina-mullite nanocomposite have been studied by Sedaghat et al. [120]. The alumina–mullite composite was prepared using sol–gel derived alumina composite nanopowders. Results revealed the intragranular mullite was embedded in the alumina grain and the intergranular mullite was embedded on the grain boundary. Accordingly, the intragranular mullite (0.3 μm) was smaller than the intergranular mullite (0.5 μm). Moreover, the alumina grains (1.0 μm) are larger than the mullite. The relative density of alumina–mullite that was sintered at 1650 °C for 2 h was obtained as 98.7%. After sintering at 1750 °C for 2 h, the mullite was decomposed.

In the other hand, mullite can be synthesized from wastes. Vieira et al. [49], have studied the mullitization kinetics from silica and alumina-rich wastes. The first were wastes from slate rocks (24.03% of Al_2O_3; main crystalline phases were muscovite, chlorite and quartz). The second were aluminum sludge's resulting from the physicochemical treatment of the wastewaters generated by aluminum surface treatment industries. Sintered products were composites of mullite and α-alumina dispersed in a glassy phase and presented flexural strengths higher than 100 MPa after sintering temperatures at 1285 °C.

4. Structure

Refractory products are highly heterogeneous ceramics, multiphase, with a coarse skeleton (aggregates; mean grain size few millimeters) connected by a matrix of fine grain size (consisting of a bond and additives). Added to these components, an additional phase consisting of the porosity (open and closed) of the ceramic, which largely contributes to fixing the thermal material properties [2]. These heterogeneities are related to the physicochemical and structural particularities of initial powders, to the grains size repartition and shape as well as to the individual transformation and interactions of components during the sintering process [109]. In general, initial compositions are selected to attain the desired performance of final products. In the case of refractory materials, porosity and mechanical strength are important parameters, which depend on the individual sintering behavior of phases, but with the interactions between phases at high temperature.

The microstructure of a silica-alumina brick elaborated from Moroccan geomaterials is shown in Fig. 6 at low and high magnifications in optic microscopy. This brick was fabricated by dry pressing of aggregates (andalusite rich schist) and a raw clay blend (kaolin clay). The use of a coarse particle size of andalusite rich schist has improved the technological quality of the refractory [109]. Considerable shrinkage of the "matrix" around coarse aggregate particles has created obvious cracks around the aggregate particles after 100 cycles of thermal choc (Fig. 6c). At higher magnification, the nature of pores in a typical fireclay brick can be seen. The elongated nature of most pores in the aggregate particle is seen along with rounded pores. The continuum of mullite and glass cannot be seen at this magnification. Etching techniques and higher magnification must be used to reveal the mullite crystals (Fig. 5).

5. Properties

Refractories are consumables materials. They are designed and manufactured so that the properties of the refractories will be appropriate for their applications. In some industries, resistance to corrosion and to abrasion may be most important while in other situations melting temperature and thermal conductivity are important. Table 3 lists the most important properties (physical,

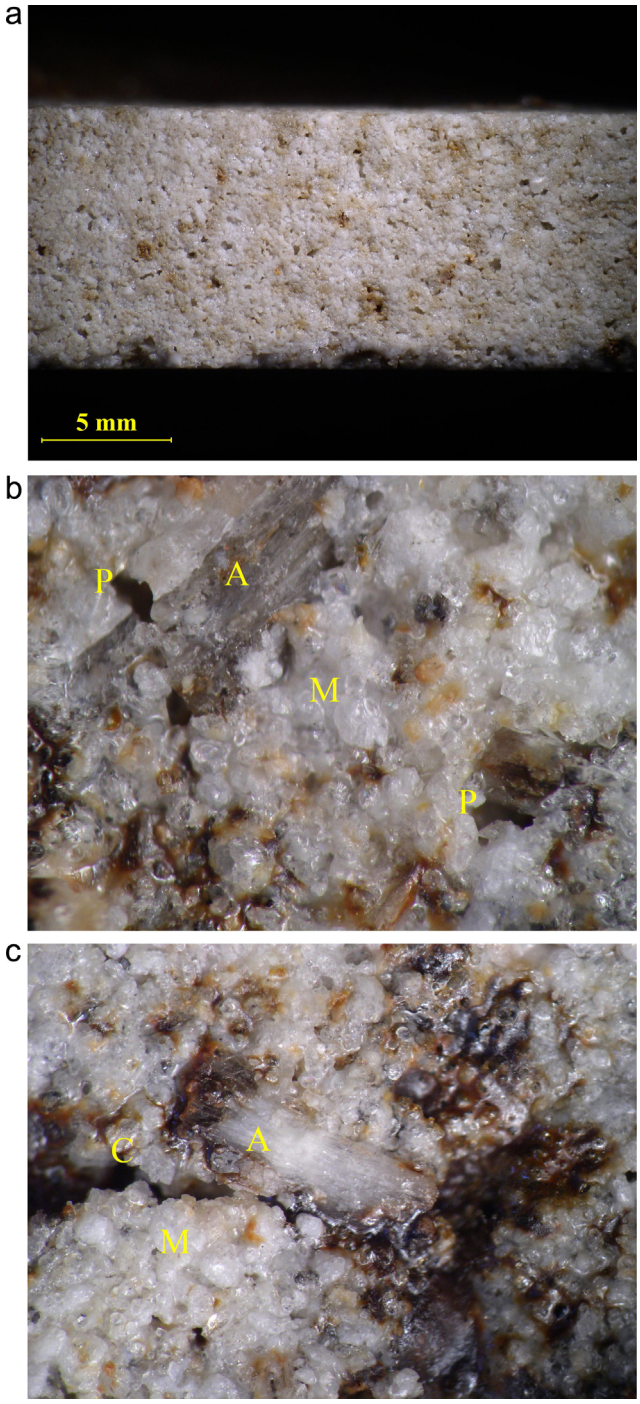

Fig. 6. Silica-alumina brick at low and high magnification. (a) Optical micrograph showing the porous structure of the firebrick fired at 1600 °C. (b) Optical micrograph at high magnification (A: Aggregates, P: Pores, M: Matrix). (c) Damage (cracking) of silica-alumina refractory fired at 1450 °C and having undergone 100 cycles of thermal shock with a temperature difference of 925 °C (A: Aggregates, C: Cracks, M: Matrix).

chemical and thermal) to be evaluated at room temperature and in service.

The apparent density, water absorption and open porosity are determined by standard methods ASTM C373-88 [122], and firing shrinkage by ASTM C 326-03 [123]. Fired products are characterized for mechanical properties like flexural strengths with three-point bending (ASTM C674-88) [124] and compressive

Table 3
Physical, mechanical, chemical and thermal characteristics for refractories materials.

Physical and mechanical characteristics	Chemical characteristics	Thermal characteristics
Density, porosity, water absorption and shrinkage	FX, XRD, SEM	Thermal conductivity and diffusivity
Distribution pore size/permeability	Corrosion/erosion	Specific heat capacity
Strength		Thermal expansion
Refractoriness under load		Thermal choc
Abrasion		Pyroscopic temperature

strength (ASTM C-133). The strength of a refractory material is an indication of its suitability for use in construction. It is a combined measure for the strength of the grains and also of the bonding system. As the major properties of the refractory materials are intimately connected to their mineralogical composition, the samples should finely crush and analyzed by X-ray diffraction. The different phases formed after firing are identified. The samples microstructures are evaluated using scanning electron (SEM) and binocular microscopy. Thermal conductivity measurements can be employed by hot-wire method (ASTM C-1113) [109]. The thermal conductivity tests are particularly important for insulating refractories where the thermal gradients from the hot face to the cold face dictate the use of a refractory material for the specific uses. The cyclic thermal shock tests are performed according to DIN 51 068 [48]. The sample are heated for 15 min at 950 °C, and immediately immersed in the cooling water at 25 °C for 3 min.

Corrosion/erosion resistance is one of the most important chemical characteristics of refractories, which are exposed to molten metal and slag. The refractories must not only resist high temperatures but also corrosion by liquid oxides. The corrosive environment usually contains liquid (melted) phases that participate in chemical reactions with the refractory at elevated temperatures resulting in refractory consumption or wear [2,3]. This corrosion involves phenomena of dissolution and precipitation of new crystalline phases [121]. However, the interpretation of the microscopic observations is difficult. Indeed, because of the crystallization of liquid glasses during cooling, the mineral phases observed at room temperature are not representative of those observed at high temperature. The microstructures of corroded refractories are very difficult to interpret because they are multi-component and heterogeneous ceramics and have complex microstructures. The microscopic observations and the analyses are carried out at room temperature. They are not representative of the mineral and vitreous phases existing at high temperature. During cooling, new solid phases appear by crystallization of liquid oxides. The composition of the vitreous phases also evolves with the temperature.

The chemical attack, the degradation mechanisms and the solid particle erosion tests of silica-alumina refractories by liquid and gas (sodium vapors, alkali-doped deposit, gas permeability) were studied [38,56,89,90,92,93]. In order to contribute to a better knowledge of this chemical attack, Prigent et al. [89], have simulate the sodium gaseous corrosion of different raw materials and refractories. Corrosion of alumina raw materials by sodium vapors is due to a dissolution–precipitation process by a Na_2O rich liquid phase. Fire clay and andalusite raw materials exhibit very high corrosion by Na vapors. Mullitized andalusite leads to excellent corrosion resistance which is close to monocrystalline fused mullite by limiting the liquid phase formation during corrosion by sodium gas. Solid particle erosion tests have been conducted by Yang et al. [92], by using sharp SiC particles between 325 and 830 μm in diameter. The impact speed is 50 m/s and the impact angle is varied between 30°

and 90°. The experimental results reveal that the alumina-based refractories exhibit increasing erosion resistance with increasing temperature and decreasing impact angle, with the minimum erosion rate at 1200 °C and 30° impact angle.

The study of the microstructures of corroded refractories was carried out by Poirier et al. [56]. The concept of local thermodynamic equilibrium and the use of the phase rule makes it possible to interpret the microstructures of corroded refractories, to explain the observed mineral zonation and to quantify the composition of the liquid phase at high temperature from chemical profiles established by SEM. Degradation mechanisms in bauxite and chamotte based bricks was studied by Stjernberg et al. [96]. The results show that potassium penetrates more deeply into the bricks than hematite, resulting in the formation of kalsilite, leucite and potassium β-alumina, which contribute to degradation of the lining. The same author studied the degradation of mullite/corundum refractories by reaction with alkali-doped deposit materials [93]. The materials tested were in both monolithic and powder form. Alkali metal carbonates (containing sodium and potassium) were used as corrosive agents, to increase reaction kinetics. XRD showed that alkali metals react with the mullite in the bricks, this being more pronounced in the case of sodium than potassium. Phases such as nepheline ($Na_2O{\cdot}Al_2O_3{\cdot}2SiO_2$), kalsilite and kaliophilite (both $K_2O{\cdot}Al_2O_3{\cdot}2SiO_2$), and leucite ($K_2O{\cdot}Al_2O_3{\cdot}4SiO_2$) were formed as a consequence of reactions between alkali metals and the refractory bricks. The formation of these phases causes volume expansions of between 20% and 25% in the brick materials, which accelerate degradation.

6. Conclusion

Refractory oxides are an important class of materials that enable processes to exploit extreme environments. In recent decades, tremendous efforts have been devoted to innovative processing of silica-alumina refractory ceramics and investigation of properties and their application in suitable fields. Because of the large number of articles in this field, this review mainly focuses on the processing and special conditions of the research works and properties of the elaborated refractory. Different processing routes for refractories ceramics have been developed for specific applications to satisfy the associated requirements for porosity, refractoriness, flexural strength and properties. In this review, the processes are divided into three categories:

- Elaboration from clay (kaolin, mixtures of clay and alumina): mullite is obtained by reaction between silica and alumina present in the clay. The firing temperature ranging between 1200 and 1400 °C.
- Elaboration from sillimanite minerals and bauxite: This type of refractory is characterized by its high refractoriness, good mechanical strength and resistance to corrosion by liquid oxides and sodium.
- Other routes: sol–gel synthesis, wastes (alumina-rich wastes, slate rocks, aluminum sludge's, ceramics wastes, etc.).

Acknowledgements

The authors acknowledge support from National Center for Scientific and Technical Research (CNRST) (research unite URAC 46) and Hassan II Academy for Sciences and Techniques (Project V2GV).

References

[1] Y. Ding, Analyse morphologique de la microstructure 3D de réfractaires électrofondus à très haute teneur en zircone: relations avec les propriétés mécaniques, chimiques et le comportement pendant la transformation quadratique monoclinique (These), Natinale School of Mines, Paris (2012).
[2] A. El Bakkali, Contribution à l'étude de la corrosion des réfractaires à base de SiC dans les cuves d'électrolyse de l'aluminium (These), University of Orléans (2009).
[3] F. Thummen, Propriétés mécaniques et durée de vie des bétons réfractaires (These), National Institute of Applied Sciences, Lyon (2004).
[4] P. Meukam, Valorisation des briques de terre stabilisées en vue de l'isolation thermique de bâtiments (These), University of Cergy Pontoise and University of Yaounde I (2004).
[5] A. Esharghawi, Élaboration de matériaux poreux à base de mullite par procédé SHS (These), University of Limoges (2009).
[6] L. Massard, Etude du fluage de réfractaires électrofondus du système alumine–zircone–silice (These), Natinale School of Mines, Paris (2005).
[7] J.M. Auvray, Elaboration et caractérisation a haute température de bétons réfractaires a base d'alumine spinelle (These), University of Limoges (2003).
[8] C. Patapy, Comportement thermomécanique et transformations de phase de matériaux réfractaires électrofondus à très haute teneur en zircone (These), University of Limoges (2010).
[9] A.G.M. Othman and N.M. Khalil, Ceram. Int., 31, 1117–1121 (2005).
[10] J. Anggono, J. Teknik. Mesin., 7, 1–10 (2005).
[11] D.A. Brosnan, Alumina-silica brick in Refractories Handbook, Ed. by C.A. Schacht, (2004) pp. 79–107.
[12] F. James, Shackelford and R.H. Doremus, Ceramic and Glass Materials: Structure, Properties and Processing (2008).
[13] T. Mah and K.S. Mazdiyasni, J. Am. Ceram. Soc., 66, 699–703 (1983).
[14] F. Gridi-Bennadji, D. Chateigner, G. Di Vitaa and P. Blanchart, J. Eur. Ceram. Soc., 29, 2177–2184 (2009).
[15] M.G.M.U. Ismail, Z. Nakai and K. Minegishi, Int. J. High. Technol. Ceram., 2, 123–134 (1986).
[16] H. Belhouchet and V. Garnier, Glass Ceram. Compos., 16–24, (2011).
[17] T. Kumazawa, S. Ohta, S. Kanzaki and Z. Nakagawa, Proc. on annual meeting ceramic society, in Extended Abstract, Tokyo, Japan, (1990) p. 34.
[18] T. Kumazawa, S. Kanzaki, S. Ohta and H. Tabata, J. Ceram. Soc. Jpn., 96, 85–91 (1988).
[19] H. Ohnishi, T. Kawanami, A. Nakahira and K. Nihara, J. Ceram. Soc. Jpn., 98, 541–547 (1990).
[20] P.F. Becher, J. Am. Ceram. Soc., 74, 255–269 (1991).
[21] S. Somiya and Y. Hirata, Am. Ceram. Soc. Bull., 70, 1624–1632 (1991).
[22] R.D. Nixon, S. Chevacharoenkul, R.F. Davis and T.N. Tiegs, J. Am. Ceram. Soc., 6, 579–603 (1990).
[23] C. Sadik, I. El Amrani and A. Albizane, MATEC Web. Conf., 2, 01016 (2012).
[24] M.A. Sainz, F.J. Serrano, J. Bastidab and A. Caballero, J. Eur. Ceram. Soc., 17, 1277–1284 (1997).
[25] A. Tomba, M.A. Camerucci, G. Urretavizcaya, A.L. Cavalieri, M.A. Sainz and A. Caballero, Ceram. Int., 25, 245–252 (1999).
[26] M.A. Sainz, F.J. Serrano, J.M. Amigo, J. Bastida and A. Caballero, J. Eur. Ceram. Soc., 20, 403–412 (2000).
[27] M. Hamidouche, N. Bouaouadja, C. Olagnon and G. Fantozzi, Ceram. Int., 29, 599–609 (2003).
[28] K. Ghanbari Ahari, J.H. Sharp and W.E. Lee, J. Eur. Ceram. Soc., 23, 3071–3077 (2003).
[29] L.B. Kong, T.S. Zhang, Y.Z. Chen, J. Ma, F. Boey and H. Huang, Ceram. Int., 30, 1313–1317 (2004).
[30] L.B. Kong, Y.Z. Chen, T.S. Zhang, J. Ma, F. Boey and H. Huang, Ceram. Int., 30, 1319–1323 (2004).
[31] V. Viswabaskaran, F.D. Gnanam and M. Balasubramanian, Appl. Clay Sci., 25, (29–35) (2004).
[32] H.B. Ramírezl, E.R. Range, E.R. Garcia and R.C. Bradt, J. Am. Ceram. Soc., 87, 144–146 (2004).
[33] L. Xu, Z. Xie, L. Gao, X. Wang, F. Lian, T. Liu and W. Li, Ceram. Int., 31, 953–958 (2005).
[34] M.L. Bouchetou, J.P. Ildefonse, J. Poirier and P. Daniellou, Ceram. Int., 31, 999–1005 (2005).
[35] T. Ebadzadeh, Ceram. Int., 31, 1091–1095 (2005).
[36] M.J. Ribeiro, D.U. Tulyagavov, J.M. Ferreira and J.A. Labrinch, J. Eur. Ceram. Soc., 25, 703–710 (2005).
[37] F.A.C. Milheiro, M.N. Freire, A.G.P. Silva and J.N.F. Holanda, Ceram. Int., 31, 757–763 (2005).
[38] S. Ueno, D. Doni Jayaseelan, N. Kondo, T. Ohji and S. Kanzaki, Ceram. Int., 31, 177–180 (2005).
[39] F.J. Torres, E.R. De Sola and J. Alarcon, J. Eur. Ceram. Soc., 26, 2285–2292 (2006).
[40] D.N. Boccaccini, C. Leonelli, M.R. Rivasi, M. Romagnoli and A.R. Boccaccini, Ceram. Int., 31, 417–432 (2005).
[41] Z. Chen, X. Zhu, Z. Liu, L. Pan and J. Tao, Ceram. Int., 32, 687–690 (2006).
[42] O. Burgos-Montes, M.I. Nieto and R. Moreno, Ceram. Int., 33, 327–332 (2007).
[43] M.F. Zawrah and M.H. Aly, Ceram. Int., 32, 21–28 (2006).
[44] E. Medvedovski, Ceram. Int., 32, 369–375 (2006).
[45] S. Maitra, A. Rahaman, A. Sarkar and A. Tarafdar, Ceram. Int., 32, 201–206 (2006).
[46] L.A. Dıaz and R. Torrecillas, J. Eur. Ceram. Soc., 27, 67–72 (2007).
[47] J.A. Santillan, H.B. Ramirez and R.C. Bradt, J. Ceram. Process. Res., 8, 1–11 (2007).

[48] M. Kolli, M. Hamidouche, G. Fantozzi and J. Chevalier, Ceram. Int., 33, 1435–1443 (2007).
[49] S.C. Vieira, A.S. Ramos and M.T. Vieira, Ceram. Int., 33, 59–66 (2007).
[50] S. Li and N. Li, Ceram. Int., 33, 551–556 (2007).
[51] T. Isobe, Y. Kameshima, A. Nakajima, K. Okada and Y. Hotta, J. Eur. Ceram. Soc., 27, 53–59 (2007).
[52] K. Prabhakaran, S. Priya, N.M. Gokhale and S.C. Sharma, Ceram. Int., 33, 515–520 (2007).
[53] J. Wang, H. Kou, X. Liu, Y. Pan and J. Guo, Ceram. Int., 33, 719–722 (2007).
[54] D.N. Boccaccini, M. Romagnoli, E. Kamseu, P. Veronesi, C. Leonelli and G.C. Pellacani, J. Eur. Ceram. Soc., 27, 1859–1863 (2007).
[55] F. Sahnoune, M. Chegaar, N. Saheb, P. Goeuriot and F. Valdivieso, Appl. Clay Sci., 38, 304–310 (2008).
[56] J. Poirier, F. Qafssaoui, J.P. Ildefonse and M.L. Bouchetou, J. Eur. Ceram. Soc., 28, 1557–1568 (2008).
[57] M. Ghassemi Kakroudi, E. Yeugo-Fogaing, C. Gault, M. Huger and T. Chotard, J. Eur. Ceram. Soc., 28, 2471–2478 (2008).
[58] M.J. Ribeiro and J.A. Labrincha, Ceram. Int., 34, 593–597 (2008).
[59] J.S. Moya, M. Diaz, C.F. Gutéerrez-Gonzalez, L.A. Diaz, R. Torrecillas and J.F. Bartolomé, J. Eur. Ceram. Soc., 28, 479–491 (2008).
[60] C.N. Djangang, A. Elimbi, U.C. Melo, G.L. Lecomte, C. Nkoumbou, J. Soro, J.P. Bonnet, P. Blanchart and D. Njopwouo, Ceram. Int., 34, 1207–1213 (2008).
[61] E. Ouedraogo and N. Prompt, J. Eur. Ceram. Soc., 28, 2867–2875 (2008).
[62] M. Awaad, M.F. Zawrah and N.M. Khalil, Ceram. Int., 34, 429–434 (2008).
[63] N. Prompt and E. Ouedraogo, J. Eur. Ceram. Soc., 28, 2859–2865 (2008).
[64] T. Ebadzadeh, M.H. Sarrafi and E. Salahi, Ceram. Int., 35, 3175–3179 (2009).
[65] G.H. Beall, J. Eur. Ceram. Soc., 29, 1211–1219 (2009).
[66] M.N. Ibarra Castro, J.M. Almanza Robles, D.A. Cortés Hernandez, J.C. Escobedo Bocardo and J. Torres, Ceram. Int., 35, 921–924 (2009).
[67] N. Rendtorff, L. Garrido and E. Aglietti, Ceram. Int., 35, 779–786 (2009).
[68] I. Ganesh and J.M.F. Ferreira, Ceram. Int., 35, 2007–2015 (2009).
[69] Z. Zivcová, E. Gregorová, W. Pabst, D.S. Smith, A. Michot and C. Poulier, J. Eur. Ceram. Soc., 29, 347–353 (2009).
[70] M. Ghassemi Kakroudi, M. Huger, C. Gault and T. Chotard, J. Eur. Ceram. Soc., 29, 571–579 (2009).
[71] M. Sutcu and S. Akkurt, Ceram. Int., 35, 2625–2631 (2009).
[72] N.M. Rendtorff, L.B. Garrido and E.F. Aglietti, Ceram. Int., 35, 2907–2913 (2009).
[73] B.M. Kim, Y.K. Cho, S.Y. Yoon, R. Stevens and H.C. Park, Ceram. Int., 35, 579–583 (2009).
[74] Y.J. Lin and S.H. Tu, Ceram. Int., 35, 1311–1315 (2009).
[75] S. Osman and C. Özgür, J. Eur. Ceram. Soc., 29, 2945–2949 (2009).
[76] A. Schrijnemakers, S. André, G. Lumay, N. Vandewalle, F. Boschini, R. Cloots and B. Vertruyen, J. Eur. Ceram. Soc., 29, 2169–2175 (2009).
[77] T.K. Mukhopadhyay, S. Ghatak and H.S. Maiti, Ceram. Int., 36, 909–916 (2010).
[78] E. Ozel and S. Kurama, Ceram. Int., 36, 1033–1039 (2010).
[79] J. Bai, Ceram. Int., 36, 673–678 (2010).
[80] C. Zanelli, M. Dondi, M. Raimondo and G. Guarini, J. Eur. Ceram. Soc., 30, 29–35 (2010).
[81] J. Stjernberg, B. Lindblom, J. Wikstrom, M.-L. Antti and M. Odén, Ceram. Int., 36, 733–740 (2010).
[82] G. Di Girolamo, C. Blasi, L. Pilloni and M. Schioppa, Ceram. Int., 36, 1389–1395 (2010).
[83] E. Garcia, J. Mesquita-Guimaraes, M.I. Osendi and P. Miranzo, Ceram. Int., 36, 1609–1614 (2010).
[84] B. Amrane, E. Ouedraogo, B. Mamen, S. Djaknoun and N. Mesrati, Ceram. Int., 37, 3217–3227 (2011).
[85] M.M. Abou-Sekkina, S.A. Abo-El-Enein, N.M. Khalil and O.A. Shalma, Ceram. Int., 37, 411–418 (2011).
[86] E. Karamanova, G. Avdeev and A. Karamanov, J. Eur. Ceram. Soc., 31, 989–998 (2011).
[87] A. Namiranian and M. Kalantar, Iran. J. Mater. Sci. Eng., 8, 29–36 (2011).
[88] N.M. Rendtorff, L.B. Garrido and E.F. Aglietti, Ceram. Int., 37, 1427–1434 (2011).
[89] P. Prigent, M.L. Bouchetou and J. Poirier, Ceram. Int., 37, 2287–2296 (2011).
[90] R.A. Rahimi, A. Ahmadi, S. Kakooei and S.K. Sadrnezhaad, J. Eur. Ceram. Soc., 31, 715–721 (2011).
[91] S. Dudczig, D. Veres, C.G. Aneziris, E. Skiera and R.W. Steinbrech, Ceram. Int., 38, 2011–2019 (2012).
[92] J.Z. Yang, M.H. Fang, Z.H. Huang, X.Z. Hu, Y.G. Liu, H.R. Sun, J.T. Huang and X.C. Li, J. Eur. Ceram. Soc., 32, 283–289 (2012).
[93] J. Stjernberg, M.A. Olivas-Ogaz, M.-L. Antti, J.C. Ion and B. Lindblom, Ceram. Int., 39, 791–800 (2013).
[94] G.I. Vazquez Carbajal, J.L. Rodriguez Galicia, J.C. Rendon Angeles, J. Lopez Cuevas and C.A. Gutiérrez Chavarria, Ceram. Int., 38, 1617–1625 (2012).
[95] E. Furlani, G. Tonello, E. Aneggi and S. Maschio, Ceram. Int., 39, 1257–1263 (2013).
[96] J. Stjernberg, J.C. Ion, M.L. Antti, L.O. Nordin, B. Lindblom and M. Odén, J. Eur. Ceram. Soc., 32, 1519–1528 (2012).
[97] M. Sutcu, S. Akkurt, A. Bayram and U. Uluca, Ceram. Int., 38, 1033–1041 (2012).
[98] A. Gungor, O. Celikcioglu and S. Sahin, Ceram. Int., 38, 4189–4194 (2012).
[99] A. Andrews and S.K.Y. Gawu, Ceram. Int., 39, 779–783 (2013).
[100] I.D. Katsavou, M.K. Krokida and I.C. Ziomas, Ceram. Int., 38, 5747–5756 (2012).
[101] A.P. Luz, M.M. Miglioli, T.M. Souza, S. Hashimoto, S. Zhang and V.C. Pandolfelli, Ceram. Int., 38, 3791–3800 (2012).
[102] M.S. Abdi and T. Ebadzadeh, Ceram. Int., 39, 1451–1454 (2013).
[103] S. Prusty, D.K. Mishra, B.K. Mohapatra and S.K. Singh, Ceram. Int., 38, 2363–2368 (2012).
[104] Y. Wang, K. Shih and X. Jiang, Ceram. Int., 38, 1879–1886 (2012).
[105] R.D. Sahnoun and J. Bouaziz, Ceram. Int., 38, 1–7 (2012).
[106] M. Sardy, A. Arib, K. Abbassi and M. Gomina, New. J. Glass Ceram., 2, 121–125 (2012).
[107] S. Martinovic, M. Vlahovic, T. Boljanac, M. Dojcinovic and T. Volkov-Husovic, J. Eur. Ceram. Soc., 33, 7–14 (2013).
[108] C. Sadik, I. El Amrani and A. Albizane, Mater. Sci. Appl., 4, 337–346 (2013).
[109] C. Sadik, I. El Amrani and A. Albizane, J. Am. Ceram. Soc., 1, 351–355 (2013).
[110] C. Sadik, I. El Amrani and A. Albizane, J. Mater. Environ. Sci., 4, 981–986 (2013).
[111] T. Isobe, M. Shimizu, S. Matsushita and Akira Nakajima, J. Am. Ceram. Soc., 1, 65–70 (2013).
[112] H. Shirasaka, T. Shimonosono, Y. Hirata and S. Sameshima, J. Am. Ceram. Soc., 1, 368–373 (2013).
[113] B. Meng and J. Peng, Ceram. Int., 39, 1525–1531 (2013).
[114] K. Boussois, S. Deniel, N. Tessier-Doyen, D. Chateigner, C. Dublanche-Tixier and P. Blanchart, Ceram. Int., 39, 5327–5333 (2013).
[115] C.Y. Bai, X.Y. Deng, J.B. Li, Y.N. Jing, W.K. Jiang, Z.M. Liu and Y. Li, Ceram. Int., 40, 6225–6231 (2014).
[116] S. Sembiring, W. Simanjuntak, P. Manurung, D. Asmi and I.M. Low, Ceram. Int., 40, 7067–7072 (2014).
[117] Y. Jing, X. Deng, J. Li, C. Bai and W. Jiang, Ceram. Int., 40, 1329–1334 (2014).
[118] I. Zake-Tiluga, R. Svinka and V. Svinka, Ceram. Int., 40, 3071–3077 (2014).
[119] N.M. Rendtorff, G. Suárez, Y. Sakka and E.F. Aglietti, Ceram. Int., 40, 4461–4470 (2014).
[120] A. Sedaghat, E. Taheri-Nassaj, G.D. Soraru and T. Ebadzadeh, Ceram. Int., 40, 2605–2611 (2014).
[121] D.A. Brosnan, Corrosion of refractories in Refractories Handbook, Ed. by C.A. Schacht, (2004) pp. 39–77.
[122] ASTM C373-88, Standard test method for water absorption, bulk density, apparent porosity, and apparent specific gravity of fired whiteware products, Glass Ceram., 15-02, (2006).
[123] ASTM C 326-03, Standard test method for drying and firing shrinkages of ceramic whiteware clays, Glass Ceram., 15-02, (2006).
[124] ASTM C674-88, Standard test methods for flexural properties of ceramic white-ware materials, Glass Ceram., 15-02, (2006).